Mar Biol (2016) 163:103
DOI 10.1007/s00227-016-2867-1

ORIGINAL PAPER

The influence of salinity on box jellyfish (*Chironex fleckeri*, Cubozoa) statolith elemental chemistry

Christopher J. Mooney[1] · **Michael J. Kingsford**[1]

Received: 23 July 2015 / Accepted: 7 March 2016 / Published online: 15 April 2016
© Springer-Verlag Berlin Heidelberg 2016

Abstract Very little is known on the sources and movements of the potentially fatal cubomedusae *Chironex fleckeri* found around estuary mouths and beaches along tropical coastlines of Australia. Largely anecdotal evidence suggests an alternating season of polyps in protected estuaries during the dry season and medusae emerging from estuaries to feed along beaches with the onset of the monsoonal season. An experiment was conducted on young wild-caught *C. fleckeri* medusae (caught at Cape York, Australia, in November 2012) to establish how elemental incorporation into statoliths was affected by salinity. A critical salinity test revealed medusae inhabit salinities >20. Medusae were held in salinities of 22, 26, 30 and 34 ($n = 5$ per treatment) for a duration of 4 days. Laser ablation inductively coupled plasma mass spectrometry was used to analyse experimental areas of statoliths and solution-based ICPMS used for analysing water samples taken from each treatment. Statolith Mg Ca^{-1} and the partition coefficient (D_{Mg}) significantly differed among treatments and were the only element Ca^{-1} ratios to do so. Multi-element Ca^{-1} signatures could also discriminate among salinity treatments. Partition coefficients revealed D_{Mg}, D_{Sr} and D_{Li} were 2.62×10^{-6}–0.81 and D_{Ba}, D_{Mn} and D_{Zn} 1.87–431. Experimental and strong correlative evidence suggested that temperature exposure and not salinity was responsible for the significant patterns seen in statolith Sr Ca^{-1} found by Mooney and Kingsford (2012). Statolith chemistry shows strong promise for determining the movement of medusae through water bodies where there are known thermal and salinity gradients.

Responsible Editor: A. Checa.

Reviewed by Undisclosed experts.

✉ Michael J. Kingsford
michael.kingsford@jcu.edu.au

[1] ARC Centre of Excellence for Coral Reef Studies, College of Marine and Environmental Sciences, James Cook University, Townsville, QLD 4811, Australia

Introduction

Chironex fleckeri is found around the mouths of estuaries and beaches along tropical coastlines of Australia and is the largest of the Cubomedusae and potentially fatal to humans. *C. fleckeri* is an active predator (Seymour et al. 2004) of prawns and fish using complex camera-type lens eyes (Nilsson et al. 2005), strong directional swimming ability (Hamner et al. 1995; Colin et al. 2013) and powerful venom (McClounan and Seymour 2012). Medusae display strong seasonality (Jacups 2010; Gordon and Seymour 2012) and widespread distribution (Tibballs 2006) and envenoming to humans can represent a significant cost to northern Australian communities in not only public health but also leisure and tourism (Bailey et al. 2003). Knowledge about *C. fleckeri* population ecology is, however, scarce (Kingsford and Mooney 2014) but see Hartwick (1991), Gordon and Seymour (2012), Kingsford et al. (2012) and Mooney and Kingsford (2012).

Hartwick (1991) suggested preferred habitats for alternating life phases of *C. fleckeri*. Like all Cubozoa, *Chironex* have a polymorphic life history with benthic asexual polyp and pelagic sexual medusa phases. Over 9 years of searching, Hartwick (1991) noticed a gradient of smaller medusae with proximity to rivers and located one annual population of polyps ~1 km from the sea in shallow subtidal water. This, coupled with medusae displaying strong seasonality with the tropical monsoon season, led Hartwick

to conclude polyps were likely in protected estuaries over the dry season and emerged as medusae to the coast with a change to monsoon season. Hartwick's (1991) suggestion evolved into the largely anecdotal paradigm of *C. fleckeri* medusae being flushed from creeks with the onset of the wet season. Elemental chemistry has the potential to determine the sources and movements of *C. fleckeri* medusae.

Elemental chemistry of calcified structures has been used in a variety of marine organisms to investigate population structure, connectivity and movement of individuals. Structures including mollusc statoliths (e.g. Zumholz et al. 2007), bivalve shells (e.g. Thébault et al. 2009), crustacean exoskeletons (e.g. Jack et al. 2011), yet most commonly fish otoliths (e.g. Campana 1999), have been investigated; all a form of calcium carbonate ($CaCO_3$), most commonly aragonite. The utility of geochemical signatures in calcified structures is based on the assumption that trace elements from surrounding waters substitute for Ca in the structure's $CaCO_3$ matrix (Zacherl et al. 2003). The use of partition coefficients can allow the evaluation of elemental discrimination in otoliths compared to the ambient water chemistry (Bath et al. 2000; Elsdon and Gillanders 2005; Tabouret et al. 2010; Walther et al. 2010). Strontium (Sr) has been found to be positively correlated with salinity, particularly evident at estuarine/marine gradients associated with coastlines, and barium (Ba) to be negatively correlated (Daverat et al. 2005; McCulloch et al. 2005; Tabouret et al. 2010). This clear close to linear relationship with salinity, defined whatever the flow regime (i.e. low flow periods, spring runoff), occurs for salinities <20 (Tabouret et al. 2010). Otolith composition has been found to reflect Sr and Ba behaviours in water (McCulloch et al. 2005; Tabouret et al. 2010) making it possible to track animals moving between salinities if the calcified structure is deposited sequentially. Upwelling-related elemental signatures can confound the interpretation of salinity-based signals (Kingsford et al. 2009). However, in nearshore waters well away from the shelf break a salinity-related signal would dominate. Cubomedusae possess a calcified structure analogous to fish otoliths, the statolith.

The cubomedusan statolith forms within the statocyst membrane at the base of the rhopalium (Fig. 1), serving to orientate the medusa (Sötje et al. 2011). Statoliths show continuous growth with concentric increments suggested to be daily in several species including the Carybdeidae *Carybdea rastonii* (Ueno et al. 1995) and the Chirodropidae *Chironex yamaguchii* (as *Chiropsalmus quadrigatus* in Kawamura et al. 2003), *Chiropsella bronzie* (as *Chiropsalmus* sp. in Gordon et al. 2004) and most recently *C. fleckeri* (Gordon and Seymour 2012). Medusan statoliths, however, are constructed of a $CaSO_4{\cdot}0.5H_2O$ (bassanite; Tiemann et al. 2006; Sötje et al. 2011) matrix, not $CaCO_3$ (usually aragonite) as for other calcified structures. These

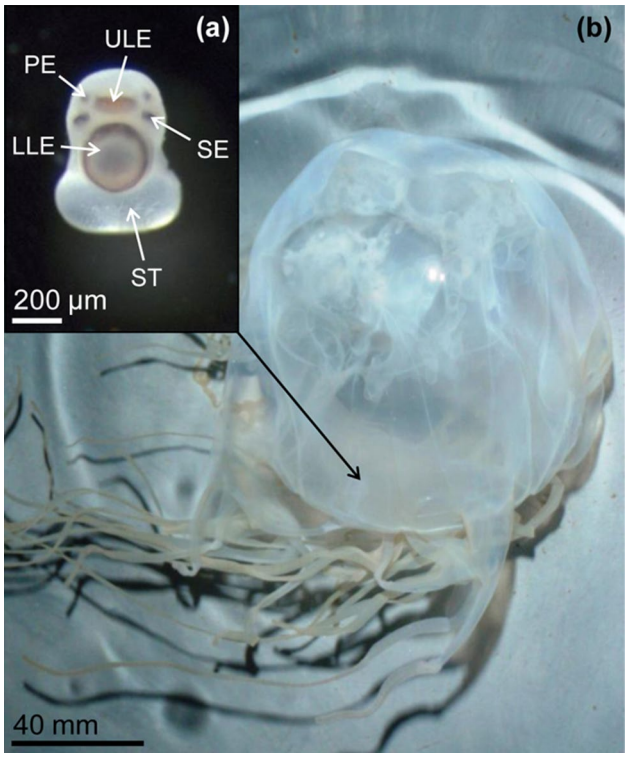

Fig. 1 (*a*) Proximal view of *C. fleckeri* rhopalium showing location of *lower* lens eye (*LLE*), pit eye (*PE*), *upper* lens eye (*ULE*), slit eye (*SE*) and statolith (*ST*) and (*b*) position of rhopalial niche on side of bell of *C. fleckeri* medusa

characteristics of *Chironex* statoliths showed great promise for elemental chemistry investigations.

Earlier research established that laser ablation inductively coupled plasma mass spectrometry (LA-ICPMS) was capable of extracting *C. fleckeri* statolith microchemistry (Mooney and Kingsford 2012). Mooney and Kingsford (2012) used Sr Ca^{-1} as a proxy for salinity to test the hypothesis that *C. fleckeri* medusae only originate from lower salinity estuaries, emerging to higher salinity coastal waters. Significant differences were found in statolith Sr Ca^{-1} between locations and strong patterns seen in statolith core to edge Sr Ca^{-1} profiles across concentric increments. Differences in Sr Ca^{-1} core to edge rankings led to the conclusion that suitable habitat for polyps is likely broader than previously thought (Mooney and Kingsford 2012). Based only on field calibration of statolith Sr Ca^{-1} matched to salinity at time of capture, experimental calibration of the relationship between Sr Ca^{-1} ratios in the bassanite statolith matrix and known salinities was required. As elemental chemistry relationships with salinity are clearest at salinities <20 (Tabouret et al. 2010), salinity survival limits of *C. fleckeri* medusae were also required.

The primary objective of this study was to experimentally calibrate how elemental ratios vary in *C. fleckeri*

statoliths among different salinities. The specific aims were as follows: (1) determine the range of salinities that *C. fleckeri* can tolerate, these data could in turn be used as the design of a calibration experiment, (2) elucidate any differences in statolith element Ca^{-1} ratios between salinities, (3) establish how this relates to water chemistry with use of partition coefficients, (4) investigate for a potential multi-elemental ratio salinity signature in statolith chemistry, and (5) perform an a posteriori comparison to determine the influence of water temperature that medusae were exposed to on statolith Sr Ca^{-1}.

Materials and methods

Sampling

Chironex fleckeri medusae were collected from Red Beach, Mapoon (12°01′6.28″S, 141°54′16.5″E), Port Musgrave, Cape York, at 0700 h, 1 November 2012. Twenty medium-sized medusae (inter-pedalial distance; IPD ≈ 40–80 mm) and 20 juvenile medusae (IPD = 12–24 mm) were collected from shallow (~0.5 m depth) tidal flats at high tide <1.5 m from a sandy beach shore near mangrove habitat. Jelly prawns (*Acetes australis*) were collected from the same location by scoop net and frozen to feed *C. fleckeri* during the experiment. A conductivity, temperature and depth device (CTD; *Seabird*, SBE 19 Plus) deployed at time of collection recorded a salinity of 33.43 and water temperature of 25.95 °C. Live medusae were transported in local sea water to the experiment location at Evans Landing, Weipa, Cape York.

Choice of salinity range

A critical salinity test was conducted on *C. fleckeri* medusae to determine a suitable salinity range for the experiment. The 20 medium-sized medusae were held in a 1000-L holding tank in sea water (salinity of 34). Dilution of holding water was achieved by the slow addition of fresh water into the holding tank. Fresh water (Weipa town water) was filtered by two 5-µm pure tec® impregnated carbon filter cartridges to reduce chlorine, bad taste and odour, sediments, pesticides, herbicides and other chemicals. Salinity was diluted at a rate of 1.42 parts h^{-1}, and periodic mixing of water was conducted with a 12 V submersible pump. The salinity of holding water was measured every 30 min with a refractometer, and observations of medusae responses were taken. The refractometer was checked for accuracy with a CTD over a range of salinities and was found to be accurate to within 0.5 parts.

Experimental design

Juvenile *C. fleckeri* medusae were used for the experiment. Four salinities: 22, 26, 30 and 34 were tested with five medusae per treatment. Our prediction of precision (standard errors of <10 % of the mean) for an n of 5 was based on the study by Mooney and Kingsford (2012). Salinities were achieved by diluting sea water collected from Albatross Bay with fresh water, through the same filtration as the critical salinity test, in 60-L bins. Acclimatisation of medusae to treatment salinities was achieved with a slow drip dilution of filtered fresh water at a rate of 1.42 parts h^{-1}. Salinities were measured with a refractometer post-mixing of water. Four water samples were taken per salinity treatment over the duration of the experiment. Samples were taken using polypropylene syringes and filtered through 0.45-µm filters into acid washed polypropylene sample jars. Water samples were then acidified to 1 % with 20 % ultrapure HNO_3 to fix the sample and enable storage.

Individual medusae were held in separate 9-L buckets in their respective salinities so that replicate jellyfish were independent. Full water exchanges were conducted bidaily, at 0600 and 1800 h, over the 4 days of experiment duration, and medusae were fed a single *A. australis* daily at noon. Buckets were randomised post-water exchange to account for potential temperature differences from one side of the experimental area to the other. Ten measurements of four random treatment buckets showed an average range of <0.5 °C (mean ± SE: 0.47 ± 0.09 °C, n = 10) across treatments. Water temperature was recorded to vary with ambient air temperature over the experimental duration and treatment water recorded every 30 min by two Tinytag TG-3100 data loggers ranged from 26.2 to 30.8 °C with a mean temperature ± SE = 28.4 ± 0.07 °C (n = 369). A natural photoperiod was maintained throughout the experiment. At the end of the 4 days, medusae were extracted from treatment salinities and preserved in 100 % ethanol.

SO-ICPMS analysis

Analysis of water samples was carried out at the Advanced Analytical Centre (AAC; James Cook University). Samples were diluted tenfold prior to trace element measurements [strontium (Sr), barium (Ba), manganese (Mn), zinc (Zn) and lithium (Li)] on a Varian 820-MS ICPMS using H_2 as a CRI gas at a flow rate of 120 mL min^{-1}. Multi-element standard solutions (1 and 5 ppb) were used to calibrate the instrument while 20 ppb of yttrium (Y) and indium (In) were added online to work as internal standards to control for instrumental drift and matrix effects. A CASS-4 sea water certified reference material (CRM) was diluted

tenfold, spiked with 1 ppb of the multi-element standard and analysed every 20 samples for quality control and used to subtract backgrounds from all analysed samples. Major elements [e.g. calcium (Ca) and magnesium (Mg)] were determined by a Varian Liberty Series II ICP-OES after trace elements analysis; a series of multi-element standard solution was used to calibrate the instrument and a 1 ppm independent standard was used as the quality control sample. Element concentrations were converted to µmol g^{-1} and ratioed to Ca (Sr Ca^{-1}; mmol mol^{-1}, Ba Ca^{-1}; µmol mol^{-1}, Mg Ca^{-1}; mmol mol^{-1}, Mn Ca^{-1}; mmol mol^{-1}, Zn Ca^{-1}; mmol mol^{-1}, Li Ca^{-1}; mmol mol^{-1}).

Statolith preparation

Analysis of element Ca^{-1} from all four statoliths of one medusa found only 2.8 % variance among the four statoliths, suggesting that a single statolith was representative for that medusa. One statolith per medusa was extracted from rhopalial tissue and placed proximal side up (cleavage vertical) in a glass petri dish. A small amount of Crystal Bond adhesive was applied to a heated slide which was then lowered onto the statolith so that it adhered. Once mounted and Crystal Bond had cooled, statoliths were polished using 0.3 µm lapping film until a transverse section displaying statolith core and smooth surface with concentric increments was visible under ×400 magnification of an Olympus CX31 compound microscope.

LA-ICPMS operation and data processing

Statoliths were analysed at the AAC (James Cook University) using a Coherent GeoLasPro excimer laser system ($\lambda = 193$ nm) coupled with a Varian 820-MS ICPMS. Statoliths were placed in a sealed sample cell mounted on an automated *X–Y* sample stage and ablation occurred in a helium (He) gas environment. A pilot study of laser operating parameters established that with a constant He gas flow rate of 240 mL min^{-1}, an energy of 80 mJ and mask aperture of 16 µm resulted in little fracturing of the bassanite statoliths, yet was capable of extracting elemental composition (see Mooney and Kingsford 2012). *C. fleckeri* statoliths grow in increments like a flattened onion. Given increments were ~6.7 µm wide and each LA pulse only drilled 0.04 µm of the bassanite statolith, we could not have confounded the 'experimental period' at the edge of the statolith with pre-experimental material. A step-repeat path was focussed around a section of the edge of the polished statolith so as to analyse the most recently deposited material. All samples were first cleaned with a step-repeat path of 1 Hz at one pulse $spot^{-1}$ with a 23 µm aperture to remove any possible etching of the surface during preparation. Then analysis was performed along the cleaned path

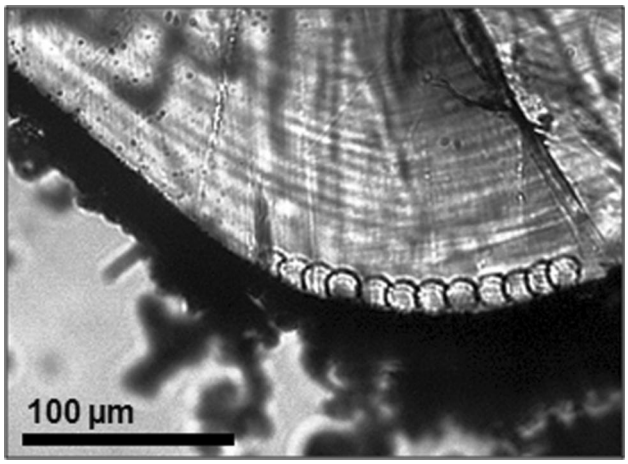

Fig. 2 Section of polished *C. fleckeri* statolith displaying concentric growth increments and 16 µm step-repeat laser ablation path around statolith edge

with a step-repeat path of 5 Hz at 10 pulses $spot^{-1}$ with 16 µm aperture (Fig. 2).

For LA-ICPMS analyses, ICPMS recording was started 30 s prior to laser ablation of each statolith sample. Statoliths were analysed for seven elements based on the following isotopes: Ca^{44}, Sr^{88}, Ba^{138}, Mg^{24}, Mn^{55}, Zn^{66}, Li^{7}. Calibration of the ICPMS was achieved using the CRM NIST 610 (National Institute of Standards and Technology, Maryland), a synthetic glass containing known levels of elements. Cleaning and analysis procedures as for statolith material were performed twice on NIST 610 before and after every eight statolith samples to correct for elemental fractionation and instrument drift in the ICPMS. The trace elements data reduction scheme (Woodhead et al. 2007) of Iolite 2.2 (Paton et al. 2011) was used for the subtraction of baselines, internal standardisation of elements to Ca and conversion of counts per second (CPS) to ppm relative to NIST 610 glass data. The Iolite parameter 'index content of Ca in sample' was set to 0.276 (Ca in $CaSO_4 \cdot 0.5H_2O$), and 'threshold to use when masking low signals' to 0 as most trace elements were only detected at very low levels. Elements were divided by their respective molar mass to produce concentrations in µmol g^{-1} and ratioed to Ca. Absolute values for elements cannot be used, as small variation in size of the laser spot can alter concentrations. In contrast, the ratioing of elemental signals (that are above detection limits) is robust given it does not vary with amount of material extracted by the laser.

Partition coefficients (D_{Me}) were calculated by dividing the element Ca^{-1} ratio measured in a statolith by the mean element Ca^{-1} ratio measured in the treatment tank water (after Morse and Bender 1990). A $D_{Me} = 1$ represents elemental deposition into the calcified structure in proportion to ambient concentrations, $D_{Me} < 1$ elemental

Table 1 Observed response of 20 *C. fleckeri* medusae resulting from sequential drops in salinity

Salinity	Observed response by medusae
34–29	Normal behaviour (regular bell pulsation, contractile tentacles, respond to stimuli)
26	Fully extended tentacles
21	All alive, bell pulsing strongly, but motionless on bottom
19	Weak pulse of bell, holding bell shape, loss of tentacle control and locomotory powers
18	Numerous tentacles detached, slight pulsing of bell, laying motionless on side
16	Loss of transparency of exumbrella, no response to stimulation, >50 % mortality

discrimination and $D_{Me} > 1$ active elemental uptake (Morse and Bender 1990).

Statistical analyses

Statistical analyses were performed using SYSTAT 11 for Windows. The model that there would be consistent differences in chemistry between salinity treatments was tested with one-way analysis of variance (ANOVA). Salinity was treated as a fixed factor (treatments: 22, 26, 30, 34). Separate ANOVAs were performed for water element Ca^{-1}, statolith element Ca^{-1} and partition coefficient (D_{Me}). Where a single extreme outlier was present for Mg Ca^{-1} in statolith chemistry, it was removed and replaced with the mean of the remaining four samples for that treatment. As a result, one degree of freedom (df) was removed from the residual for Mg Ca^{-1} in ANOVA for statolith chemistry and corresponding D_{Mg} following the procedures of Underwood (1997). Water chemistry and statolith chemistry data were log-transformed to satisfy the assumption of normality. Variances among treatments were not all homogeneous, yet fortunately ANOVA is robust and capable of operating well even with considerable heterogeneity of variances as long as all *n* are equal (Glass et al. 1972).

An a posteriori power analysis (*n* required for power of 80 %) was completed on element Ca^{-1} ratios which demonstrated a strong, but not significant trend with changing salinity treatments following procedures recommended by Cohen (1988). The one-way analysis required the means by treatment (required to determine the effect size) and the average SD within groups from the experiment.

Multivariate techniques were applied to statolith chemistry to test for a multi-element signature that could differentiate among the salinities which experimental medusae had experienced. Principal component analysis (PCA) determined that log (Ba Ca^{-1}), log (Mg Ca^{-1}) and log (Zn Ca^{-1}) were responsible for describing the most variance between salinity treatments. Following this, canonical discriminant analysis (CDA) with a 'leave one out' cross-validation jackknifed classification procedure was performed on statolith log (Ba Ca^{-1}), log (Mg Ca^{-1}) and log (Zn Ca^{-1}) to determine the robustness of elemental signatures to predict the salinities to which medusae were exposed.

Statolith Sr Ca^{-1} versus water temperature

An a posteriori comparison was made of statolith Sr Ca^{-1} and water temperature to determine any affect that the water temperature medusae were exposed to had on the incorporation of Sr Ca^{-1} into statoliths. Whole statolith Sr Ca^{-1} from medusae collected from the Strand, Townsville, Queensland, Australia, over four seasons spanning 2008/2009–2011/2012 was compared to the mean water temperature measured at Middle Reef (Townsville) for 2 months prior to the collection of medusae (based on Australian Institute of Marine Science data). Further, Sr Ca^{-1} in the statoliths of medusae treated with a salinity of 34 and held at a constant temperature over 4 days was compared. Sr Ca^{-1} of the statolith edges from medusae from the 2010 field calibration at Wooldrum Point was also compared to mean water temperature over 3 days of the field calibration (from Mooney and Kingsford 2012). Five medusae from each source were used in the least squares regression to test the dependence of statolith Sr Ca^{-1} on water temperature.

Results

Critical salinity test

The behaviour of *C. fleckeri* was normal to a salinity of 26 (Table 1). Tentacles remained extended before medusae lay on the substratum at salinities just above 20. At salinities ≤~20, *C. fleckeri* medusae ceased moving, until the dilution was ceased at a salinity of 16 as >50 % mortality was observed (Table 1). Accordingly, a salinity range of 22–34 was chosen for the experiment.

Water chemistry

The concentrations of single elements generally increased with salinity across the tested range, as would be predicted. In contrast, Mn showed little change among treatments from a salinity of 22–30 with a slight decrease at 34. There was a strong trend where Zn declined with an increase in salinity. However, once ratioed to Ca different patterns were observed.

Table 2 ANOVA results of log (element Ca^{-1}) ratios for (a) water chemistry (a = 4, n = 4, F-crit = 3.49), (b) statolith chemistry (a = 4, n = 5, F-crit = 3.24; Mg Ca^{-1} = *3.29*) and (c) partition coefficient D_{Me} (a = 4, n = 5, F-crit = 3.24; Mg Ca^{-1} = *3.29*)

	Source	*df*	MS	*F*
(a)				
Sr Ca^{-1}	S	3	0.001	0.660
	R	12	0.002	
Ba Ca^{-1}	S	3	0.008	2.338
	R	12	0.004	
Mg Ca^{-1}	S	3	1.00×10^{-5}	0.193
	R	12	5.00×10^{-5}	
Mn Ca^{-1}	S	3	0.068	2.384
	R	12	0.029	
Zn Ca^{-1}	S	3	1.194	336.310***
	R	12	0.004	
Li Ca^{-1}	S	3	0.001	0.838
	R	12	0.001	
(b)				
Sr Ca^{-1}	S	3	0.008	1.908
	R	16	0.004	
Ba Ca^{-1}	S	3	0.505	1.348
	R	16	0.374	
Mg Ca^{-1}	S	3	4.302	14.517***
	R	15	0.296	
Mn Ca^{-1}	S	3	0.105	0.332
	R	16	0.315	
Zn Ca^{-1}	S	3	0.242	0.863
	R	16	0.280	
Li Ca^{-1}	S	3	0.043	0.190
	R	16	0.228	
(c)				
D_{Sr}	S	3	0.009	1.710
	R	16	0.005	
D_{Ba}	S	3	0.769	1.668
	R	16	0.461	
D_{Mg}	S	3	0.305	14.513***
	R	15	0.021	
D_{Mn}	S	3	0.078	0.637
	R	16	0.123	
D_{Zn}	S	3	0.191	0.749
	R	16	0.254	
D_{Li}	S	3	0.179	0.180
	R	16	0.995	

S salinity, *R* residual

*** $P < 0.001$

There was little variation in Sr Ca^{-1}, Mg Ca^{-1} and Li Ca^{-1} with increases in salinity, while Ba Ca^{-1}, Mn Ca^{-1} and Zn Ca^{-1} showed negative trends. Zn Ca^{-1} significantly declined in water as salinity increased (Table 2a; Fig. 3). No other element Ca^{-1} significantly differed among treatments (Table 2a). Mean Ba Ca^{-1} had a strong trend with a stepped drop across treatments as salinity increased, with highest Ba Ca^{-1} values at a salinity of 22, dropping down from 26 to 30, and lowest values were found at 34 (Fig. 3). Mn Ca^{-1} was found at much lower levels and also declined with increase in salinity from a mean of 0.039–0.019 mmol mol^{-1} (Fig. 3). Sr Ca^{-1} values were consistently around 8 mmol mol^{-1} across the tested salinity range with a trend for slight decrease at salinity of 34, but this was not significant (Fig. 3; Table 2a). Mg Ca^{-1} was about 5700 mmol mol^{-1} for all four salinity treatments, while Li Ca^{-1} displayed a similar trend to Sr Ca^{-1}, staying at a stable level from salinity 22–30 around 3 mmol mol^{-1} with a slight decline at salinity of 34; these differences were not significant (Fig. 3; Table 2a).

Statolith chemistry

Significant differences in Mg Ca^{-1} were found with changes in salinity (Table 2b). Mg Ca^{-1} was barely detected at low salinity (i.e. mean at salinity 22 ± SE = 0.06 ± 0.02 mmol mol^{-1}, n = 5; mean at salinity 26 ± SE = 0.01 ± 0.01 mmol mol^{-1}, n = 5), but high levels were detected at salinity 34 (mean ± SE = 3.59 ± 2.14 mmol mol^{-1}, n = 5; Fig. 3). Other elements Ca^{-1} showed some strong trends among salinity treatments (e.g. Ba Ca^{-1} and Zn Ca^{-1}), but variation among replicates was high and no significant differences with salinity were detected (Table 2b). There was a strong trend for Ba Ca^{-1} to increase with salinity among treatments from mean ± SE = 17.83 ± 11.88 µmol mol^{-1} (n = 5) at salinity of 22 to mean ± SE = 120.11 ± 65.55 µmol mol^{-1} (n = 5) at 34 (Fig. 3). However, standard errors were 36–67 % of the mean and differences were not significant (Table 2b). Mean Zn Ca^{-1} showed a similar trend and increased sharply with salinity, with a marked step up from salinity 30–34 (Fig. 3). Mean statolith Sr Ca^{-1} did not increase with salinity across the tested treatments, ranging between 2.30 and 2.84 mmol mol^{-1} for the four treatments (Fig. 3). Differences among treatments were not significant and there was no discernable 'effect size' from lowest to highest salinities (Table 2b). The lack of a response with salinity could not be explained by a lack of precision as standard errors were only 3.5–11.5 % of the mean. Mean statolith Mn Ca^{-1} increased in a step function from salinity 22–26 and although within treatment variances were again high (SE = 49–59 % of the mean) values plateaued at higher salinities (Fig. 3). Li Ca^{-1} values were characterised by similar mean values among treatments and high within treatment variation (SE = 33–62 % of the mean; Fig. 3).

There was a risk of type II error for elements that were not significantly different but showed a trend with salinity.

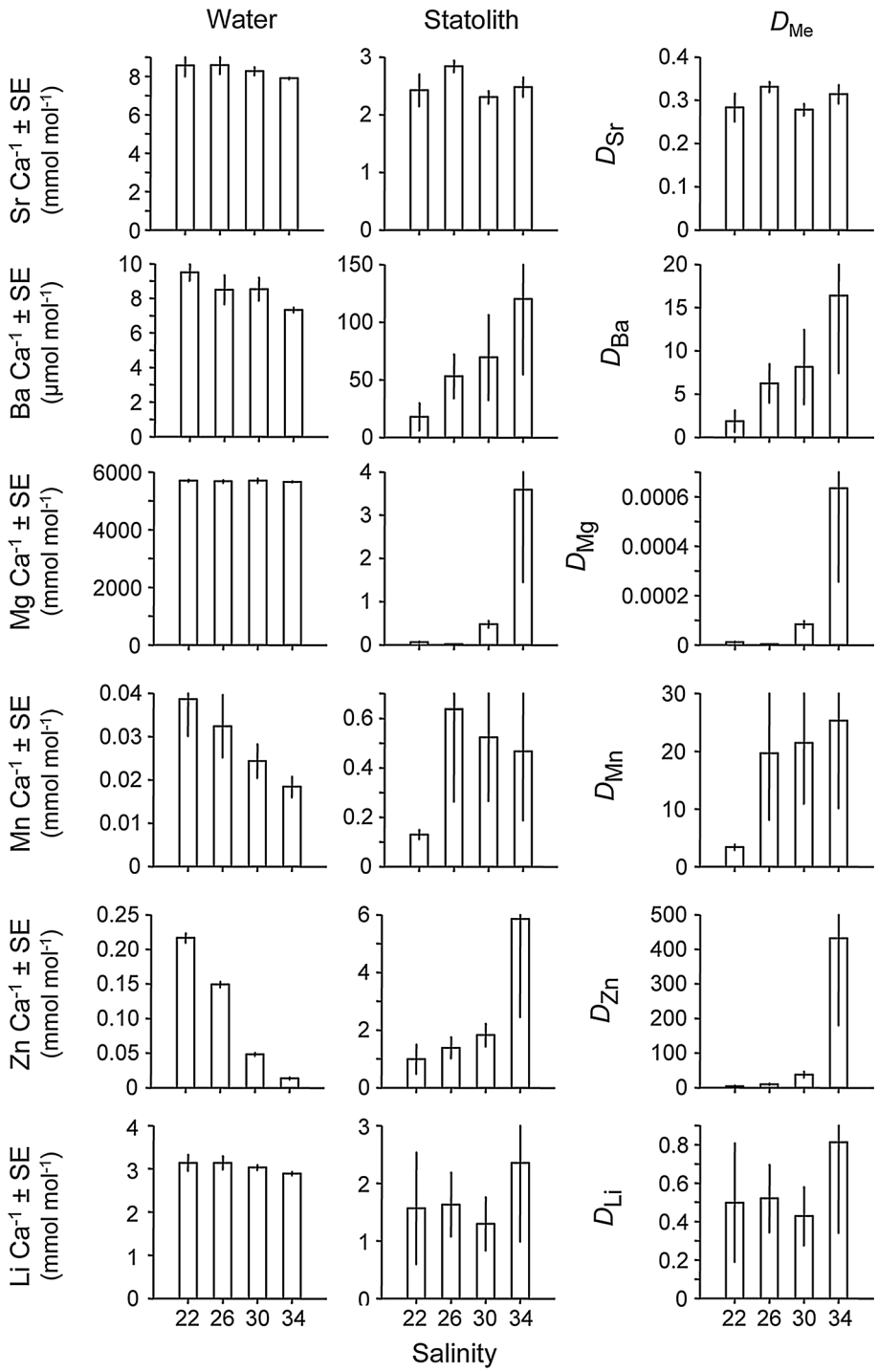

Fig. 3 Mean element Ca^{-1} ratios (±SE) for experimental water, experimental zone of *C. fleckeri* statolith, and ratio partition coefficient (D_{Me}) across salinity treatments

Power analyses performed on Ba Ca^{-1} and Zn Ca^{-1} demonstrated that for an 80 % chance of rejecting the null hypothesis if it was false, it would have required large sample sizes (i.e. Ba Ca^{-1} would require $n = 14$ and Zn Ca^{-1} $n = 20$).

Partition coefficients

There were also strong trends for partition coefficients (D_{Me}) among salinity treatments and these largely reflected the relationships found for element Ca^{-1} ratios (Fig. 3).

D_{Mg} significantly differed among salinities, mirroring patterns seen in statolith Mg Ca^{-1}; no other significant differences were detected between salinity treatments (Table 2c). D_{Mg}, D_{Sr} and D_{Li} were all <1 ranging from 2.62×10^{-6}–0.81, and D_{Ba}, D_{Mn} and D_{Zn} were all >1 ranging from 1.87 to 431 (Fig. 3); high values indicated that uptake increased greatly at high salinities.

Multivariate salinity signature

Multi-element Ca^{-1} signatures could successfully assign samples to their salinity treatment (CDA performed on statolith log (Ba Ca^{-1}), log (Mg Ca^{-1}) and log (Zn Ca^{-1}); Wilks Lamda = 0.160, $F_{(9,34)} = 4.262$, $P = 0.009$; Fig. 4). Salinity treatments of 22–30 had best classification with an overall chance of 60–80 % correct classification following jackknifed cross-validation (Table 3).

Statolith Sr Ca^{-1} versus water temperature

A strong positive relationship was detected between statolith Sr Ca^{-1} and water temperature (Fig. 5, linear regression: $r^2 = 0.54$, $F_{(1,28)} = 33.28$, $P < 0.001$). Regression analysis and associated ANOVA tests demonstrated that the slope was significantly different from zero and the relationship explained 54.3 % of the variation.

Discussion

Chironex fleckeri could not tolerate salinities of ≤~20. Accordingly, salinities of 22, 26, 30 and 34 are a representative range of the full range of salinities that wild *C. fleckeri* medusae can endure. These findings were not only of utility with respect to the planning of the experiment, but are of utility to be used for models that predict the occurrence of *C. fleckeri*. For example, Kingsford et al. (2012) concluded that numbers of *C. fleckeri* drop off quickly along the tropical coast of northern Australia during periods of heavy rain and riverine runoff. The experimental data, therefore, provide a causal mechanism for this drop off.

We initially placed some emphasis on statolith Sr Ca^{-1} as a strong potential discriminator of salinity (e.g. Mooney and Kingsford 2012), but we quickly established that *C. fleckeri* medusae are moribund or dead at salinities of <20. As major variations in Sr Ca^{-1} in water occur at salinities <15 (Phillis et al. 2011), analyses of other element Ca^{-1} ratios played a greater role than we initially predicted.

Mg Ca^{-1} was the only element Ca^{-1} to significantly vary within statoliths among salinity treatments. Few studies have focussed on the incorporation of Mg into calcified structures as a result of changes in salinity. Investigations into aragonitic fish otoliths have found otolith Mg Ca^{-1} was

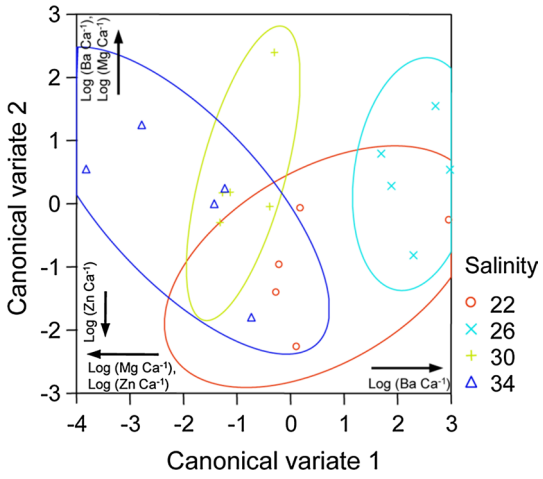

Fig. 4 Canonical discriminant analysis of *C. fleckeri* statolith log (Ba Ca^{-1}), log (Mg Ca^{-1}) and log (Mn Ca^{-1}) for four salinity treatments. Canonical Variate (CV) 1 = 87.9 %, CV 2 = 12.2 %. *Ellipses* confidence around group data. Individual elemental ratio loadings are indicated for each CV

Table 3 Canonical discriminant analysis classifications based on log (Ba Ca^{-1}), log (Mg Ca^{-1}) and log (Mn Ca^{-1}) of *C. fleckeri* statolith experimental zone for four salinity treatments

Salinity	% correct classification	Salinity classified to following jackknifed classification (% of samples)			
		22	26	30	34
22	**80**	**60**	20	20	
26	**100**	40	**60**		
30	**80**			**80**	20
34	**40**	20		40	**40**

$n = 5$ per treatment; bold = correctly classified

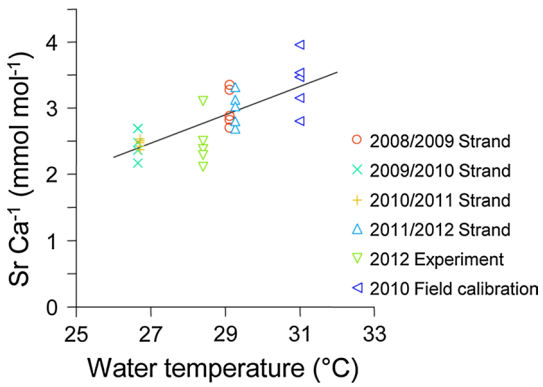

Fig. 5 Sr Ca^{-1} in *C. fleckeri* statolith versus water temperature. Sr Ca^{-1} = whole statolith for four seasons from the Strand, Townsville, Australia; statolith edge for 2012 Experiment and 2010 field calibration. Water temperature = mean of 2 months prior to medusae collection for four seasons from the Strand; mean over 4 days for 2012 Experiment; mean over 3 days for 2010 field calibration

not affected by salinity, yet have focussed only on salinities <32 (e.g. juvenile spot *Leiostomus xanthurus*; Martin and Thorrold 2005 and flathead mullet *Mugil cephalus*; Wang 2014). Similar non-significant results were found for Mg Ca^{-1} in aragonitic soft shell clams (*Mya arenaria*; Strasser et al. 2008). However, a general trend has been found in Mg Ca^{-1} in calcite of foraminifera for Mg Ca^{-1} to increase with increases in salinity, and this was particularly evident in higher salinity ranges ~≥36 (Ferguson et al. 2008). Similar to the foraminifera, it appears that Mg Ca^{-1} increases at higher salinity ranges in Cubozoa bassanite statoliths (i.e. salinity 34 treatment), and thus will be a good discriminator of exposure to full sea water (≥salinity 34) or lower salinity estuarine waters in *C. fleckeri*. Mg is super abundant in sea water compared to requirements of many marine taxa, and therefore, its uptake and levels in body fluids and flesh are highly regulated (Watanabe et al. 1997). D_{Mg} was considerably less than one with a maximum mean value of 0.00063. Water Mg Ca^{-1} was consistently high for all four salinity treatments but statolith Mg Ca^{-1} showed very low levels at salinities of 22 and 26 and then increased sharply as salinity treatment increased. D_{Mg} was also found to be much less than one in aragonitic otoliths of *L. xanthurus* (Martin and Thorrold 2005). It was suggested by Martin and Thorrold (2005) that Mg ions were actively excluded from the otoliths and that this occurred either during movement across membranes or in the endolymph at the site of aragonite precipitation. Branchial, intestinal or endolymphatic membranes isolate otoliths from sea water (Campana 1999), so physiological processes also influence otolith composition, and fish obviously control ion transport across membranes for osmoregulatory purposes (Martin and Thorrold 2005). Cubomedusan statolith formation occurs within the statocyst which consists of epidermis, mesoglea and gastrodermal cells (Sötje et al. 2011). It is unclear at which stage regulation of ions is occurring, but the very low values of D_{Mg} clearly demonstrated that this is happening.

No other element Ca^{-1} ratio significantly varied among salinity treatments. However, Ba Ca^{-1} and Zn Ca^{-1} showed strong trends across treatments with some potential to be useful in determining local population level movements among salinities, but only with large sample sizes (i.e. *n* of 14–20) for a high probability of detection. Large numbers of *C. fleckeri* of similar size are very difficult to find in the field. The lack of sensitivity for these elements also suggests that the ability of these standalone ratios to reconstruct (i.e. elemental profiles from the core) the salinity-based environmental conditions that individual jellyfish experience would be weak.

Barium was incorporated into *C. fleckeri* bassanite statoliths at greater levels than some marine fish aragonite otoliths or even cuttlefish aragonite statoliths. At a salinity of 34, mean *C. fleckeri* statolith Ba Ca^{-1} of 120 µmol mol^{-1} and D_{Ba} of 16.40 far exceeded examples of 15.8 µmol mol^{-1} in aragonitic *L. xanthurus* otoliths (Martin and Thorrold 2005) and ~16 µmol mol^{-1} reported in aragonitic cuttlefish (*Sepia Officinalis*) statoliths (Zumholz et al. 2007), or D_{Ba} of 0.043 in European eel (*Anguilla anguilla*; Tabouret et al. 2010), 0.21 in a tropical damselfish (*Acanthochromis polyacanthus*; Walther et al. 2010) and 0.27 in black bream (*Acanthopagrus butcheri*; Elsdon and Gillanders 2005) aragonite otoliths. Although mean statolith Ba Ca^{-1} and D_{Ba} increased across treatments of the current study, differences between salinities were not significant. A clear negative relationship with salinity and Ba Ca^{-1} is most apparent at salinities <20 (Tabouret et al. 2010). Some variations in Ba Ca^{-1} could be found over salinities 20–35 but appeared very small when compared to observed gradients between freshwater and sea water end members (Tabouret et al. 2010). As *C. fleckeri* medusae only inhabit waters within the higher salinity interval >20, it is no surprise that differences in statolith Ba Ca^{-1} were not significant. Aragonitic otolith Ba Ca^{-1} has been found to be a useful proxy for salinity gradients (at salinities 4–23) in sole (*Solea solea*; Tanner et al. 2013) and salinity affected D_{Ba} in spot (*L. xanthurus*; Bath et al. 2000; Martin and Thorrold 2005), yet Ba Ca^{-1} had no significant relationship with salinity in aragonitic statoliths of cuttlefish (*S. officinalis*; Zumholz et al. 2007).

Water Zn Ca^{-1} was found to significantly differ between salinity treatments displaying a distinct decline in levels as salinity increased (Table 2a; Fig. 3). Determination of Zn by solution-based ICPMS (SO-ICPMS) is difficult mainly due to sea water salts giving complicated interferences on all Zn isotopes for which the quadrupole ICPMS is unable to resolve (pers comm Hu at AAC). As high Zn background levels can also hamper Zn determination in sea water samples, results for water Zn Ca^{-1} should be treated with caution. Despite this, there was a strong but not significant trend for statolith Zn Ca^{-1}, and more drastically D_{Zn}, to increase with salinity. Mean D_{Zn} was over 400 at the highest salinity treatment of 34. A possible explanation could be that adsorption of elements may increase at lower ambient concentrations, while binding sites become saturated as elemental concentrations rise and equilibrium is reached in the solution interface and growing crystal surface (Watson 1996). Another possible explanation was suggested by Templeman and Kingsford (2010) when Zn concentrations were found at high levels in tissue of the scyphozoan *Cassiopea* sp. even though Zn concentrations in ambient sea water were below detection limits. Templeman and Kingsford (2010) suggested that *Cassiopea* sp. was efficient at either obtaining Zn from their food or water, or recycling Zn. The exact mechanism in *C. fleckeri* is not known, but the ability to accumulate Zn probably limits the utility of

Zn as a standalone discriminator of the conditions that jellyfish experience.

The remaining element Ca^{-1} ratios showed little potential for discrimination between conditions experienced, either actively regulating or accumulating elements. Mn Ca^{-1} showed no consistent pattern across salinity treatments. Mean D_{Mn} were >1, reaching up to 25.33 at salinity 34. Mn was found to accumulate more than ten times above ambient sea water concentrations in tissue of the scyphozoan *Cassiopea* sp. (Templeman and Kingsford 2010), and up to 100 times greater than typical sea water concentrations in tentacles of the scyphozoan *Pelagia noctiluca* (Cimino et al. 1983). Mn is perhaps an essential element for medusae existence. Li Ca^{-1} also showed no apparent pattern across the tested salinity treatments. D_{Li}, however, was <1, indicating elemental discrimination. Templeman and Kingsford (2010) found Li to be the only element present at lower tissue concentrations than ambient sea water concentration in *Cassiopea* sp., suggesting Li to be actively regulated within the body although mechanisms and requirements for regulation were not known. Li is perhaps quite the opposite of Mn and a non-essential element for medusae existence.

Statolith Sr Ca^{-1} did not increase across the tested salinity treatments and this was partly because *C. fleckeri* medusae die before they can be exposed to low salinities (i.e. <20). Furthermore, Sr Ca^{-1} did not significantly differ between salinity treatments in water, statoliths or partition coefficient. The incorporation of Sr into *C. fleckeri* bassanite statoliths was, however, found to be directly comparable to several studies on fish otoliths that are made of $CaCO_3$ (usually aragonite). Mean D_{Sr} ranged between 0.28 and 0.33 across the four salinity treatments. This range is equivalent to mean D_{Sr} of 0.28 seen in black bream (*A. butcheri*) otoliths (De Vries et al. 2005), 0.29 recorded in spot (*L. xanthurus*) otoliths (Martin et al. 2004), 0.31 in striped bass (*Morone saxatilis*; Phillis et al. 2011) and 0.33 in eel (*A. Anguilla*; Tabouret et al. 2010). If D_{Sr} is so similar in *C. fleckeri* statoliths and some fish otoliths, why was no positive correlation between statolith Sr Ca^{-1} and salinity detected?

Chironex fleckeri medusae inhabit estuarine and coastal waters of salinity >20. Major changes in Sr Ca^{-1} occur at salinities <15 (Phillis et al. 2011) and the clear close to linear positive relationship that can be seen between Sr Ca^{-1} and salinity occurs for salinities <20 (Tabouret et al. 2010). Element Ca^{-1} ratios have been found to be almost constant at salinities between 20 and 25 (Kraus and Secor 2004; Elsdon and Gillanders 2005; Tabouret et al. 2010). Elsdon and Gillanders (2005) found salinity was not correlated with ambient Sr Ca^{-1} in estuarine locations sampled, and Miles et al. (2009) found it difficult to discriminate estuarine conditions when examining movements between fresh water and sea water for five Australian riverine fishes. Indeed in most systems, Sr Ca^{-1} is said to be best suited to determine between fresh water and more saline waters (Phillis et al. 2011), not solely estuarine waters. We demonstrated that *C. fleckeri* medusae will only likely survive in higher salinity estuarine and coastal waters (Table 1); it is understandable, therefore, why statolith Sr Ca^{-1} was not significantly affected by salinity. Salinity is obviously not the explanation for the strong significant patterns found in *C. fleckeri* statolith Sr Ca^{-1} (Mooney and Kingsford 2012).

There was strong correlative evidence that temperature rather than salinity was a primary driver in altering the Sr Ca^{-1} values in *C. fleckeri* statoliths. Temperature has a strong and significant effect on Sr incorporation in aragonitic fish otoliths (Bath et al. 2000; Martin et al. 2004) and corals (Marshall and McCulloch 2002). It is highly likely that variation in temperature caused the variation in Sr Ca^{-1} that was found in the bassanite statoliths of wild *C. fleckeri* (Mooney and Kingsford 2012). The a posteriori comparison between statolith Sr Ca^{-1} and water temperature that medusae were exposed to found a significant positive relationship—as water temperature rose, so too did statolith Sr Ca^{-1} (Fig. 5). Relationships between temperature and Sr Ca^{-1} in the aragonite from animals of different taxa vary; positive (Bath et al. 2000; Martin et al. 2004), negative (Sadovy and Severin 1992; Secor et al. 1995) and no effect have been found (Gallahar and Kingsford 1996; Tzeng 1996). Sr Ca^{-1} in cuttlefish (*S. officinalis*) statoliths was found to show no relationship to salinity or temperature (Zumholz et al. 2007). Additional calibration experiments are required and would help to test our prediction that temperature affects Sr incorporation into *C. fleckeri* bassanite statoliths.

There are few other factors that are likely to cause large changes in Sr Ca^{-1} in Ca-based structures. Some elements can be accrued through the diet (Sanchez-Jerez et al. 2002), but *C. fleckeri* diet is thought to be similar among locations (i.e. prawns and small fish; Carrette et al. 2002). Although levels of Sr isotopes that contribute to the elemental signatures can vary in fresh water (e.g. based on source rocks with drainage systems), the isotopic composition of Sr in saltwater is very stable (McCulloch et al. 2005). Accordingly, we suggest that greatest variation in Sr Ca^{-1} at salinities above 20 would be from temperature.

In this study, salinity was varied and care was taken to keep diet, photoperiod and temperature consistent among treatments. Furthermore, the temperatures experienced by experimental medusae were similar to the daily range found in coastal habitats occupied by medusae. Comparisons among salinities were also not confounded with ontogenetic stage as all individuals were of a similar size and number of tentacles. Moreover, we did not confound sampling on bassanite that was outside of the experimental

period as sampling pits were tiny when compared to width of statolith increments. Assuming that *C. fleckeri* growth increments in statolith are daily (Gordon and Seymour 2012), the analysed section of statolith material would equate to ~2.4 days (Mooney and Kingsford 2012), well within the 4 days of salinity treatment exposure.

Templeman and Kingsford (2012) published elemental concentrations of *C. fleckeri* bell tissue. Element Ca^{-1} ratios calculated from mean tissue concentrations of standalone elements (after Table 2; Templeman and Kingsford 2012) showed similar levels to either water or statolith element Ca^{-1} of the current study. Templeman and Kingsford (after 2012) reported tissue Sr Ca^{-1} = 9.66 mmol mol^{-1} which relates much closer to water concentrations than statolith concentrations of the current study. Interestingly, statoliths from the same three medusae assessed by Templeman and Kingsford (2012) were those from Cardwell in Mooney and Kingsford (2012) where mean ± SE statolith edge Sr Ca^{-1} = 3.32 ± 0.23 mmol mol^{-1} (n = 3), three times lower than tissue values, suggesting some form of active Sr regulation between *C. fleckeri* bell tissue and statolith matrix. Tissue Mg Ca^{-1} = 5392.15 mmol mol^{-1} (after Templeman and Kingsford 2012) is much closer to water Mg Ca^{-1} than statolith Mg Ca^{-1} of the current study, also suggesting heavy regulation of Mg somewhere between bell tissue and statolith formation. Tissue Ba Ca^{-1} = 21.94 µmol mol^{-1}, Mn Ca^{-1} = 0.18 mmol mol^{-1}, Zn Ca^{-1} = 1.42 mmol mol^{-1} and Li Ca^{-1} = 1.96 mmol mol^{-1} (after Templeman and Kingsford 2012) are all within the ranges of statolith element Ca^{-1} found within the current study, suggestive of near equilibrium between *C. fleckeri* bell tissue and statolith concentrations for these element Ca^{-1} ratios. Templeman and Kingsford (2012) also presented data on several scyphomedusae and one other cubomedusae and concluded that the accumulation of elements in tissues is likely to vary by species, uptake route, speciation of the metal and organism sensitivity.

Multivariate (MV) salinity signatures [using log (Ba Ca^{-1}), log (Mg Ca^{-1}) and log (Zn Ca^{-1})] were found within *C. fleckeri* statoliths across the tested range. Highest success in classification of samples post-cross-validation was at salinities lower than 30 with low successful classification at salinity 34. MV salinity signatures in statolith chemistry thus show potential to distinguish exposures of wild medusae to water masses of different salinities and these MV signatures could complement the standalone Mg Ca^{-1} levels in *C. fleckeri* statoliths. Where Mg Ca^{-1} could delineate between exposure to full sea water of salinities ≥34 and lower salinity estuarine waters, the MV signature can delineate at a finer scale among the estuarine salinities. Given the tight salinity gradient *C. fleckeri* medusae inhabit, reconstructing movements among salinities would be of highest utility where known salinity gradients exist. The experimental findings and a posteriori comparisons with field studies strongly indicated that temperature rather than salinity will influence Sr Ca^{-1} profiles and therefore can be used to map thermal variation within local populations (sensu Kingsford and Mooney 2014) and help to resolve local movements in the wild populations.

Conclusions

Chironex fleckeri medusae became immobile and quickly died at salinities <20; this suggests a hidden vulnerability to strong riverine runoff (Kingsford et al. 2012) that had not been demonstrated experimentally until this study. Statolith Mg Ca^{-1}, D_{Mg} and multi-element Ca^{-1} signatures varied significantly at salinities from 22 to 34. Although there were some strong positive trends, no other element Ca^{-1} varied significantly among treatments. Partition coefficients were element dependent: D_{Sr}, D_{Mg} and D_{Li} were all <1 indicating elemental discrimination and D_{Ba}, D_{Mn} and especially D_{Zn}, were >1, some far exceeding values recorded in $CaCO_3$ structures, indicating active elemental uptake. There was strong correlative evidence the Sr Ca^{-1} patterns seen in *C. fleckeri* statoliths (Mooney and Kingsford 2012) relate to changes in temperature and not salinity. Reconstruction of medusa movements by statolith elemental chemistry has high potential where there is a known salinity and temperature gradient. Further experiments are required to confirm the utility of statolith chemistry as a tool for reconstructing medusa movements.

Acknowledgments We would like to thank volunteers Mark O'Callaghan and Avril Underwood for assistance in Weipa, Yi Hu at AAC for assistance with SO-ICPMS and Townsville Lifeguard Service for provision of some statoliths from the Strand, Townsville. This research was supported by a grant from the Australian Lions Foundation to CJM. We also thank Queensland Boating and Fisheries Patrol, Fisheries Queensland for use of their Evans Landing facility to conduct the experiment.

References

Bailey PM, Little M, Jelinek GA, Wilce JA (2003) Jellyfish envenoming syndromes: unknown toxic mechanisms and unproven therapies. Med J Aust 178:34–37

Bath GE, Thorrold SR, Jones CM, Campana SE, McLaren JW, Lam JWH (2000) Strontium and barium uptake in aragonitic otoliths of marine fish. Geochim Cosmochim Acta 64:1705–1714. doi:10.1016/S0016-7037(99)00419-6

Campana SE (1999) Chemistry and composition of fish otoliths: pathways, mechanisms and applications. Mar Ecol Prog Ser 188:263–297. doi:10.3354/meps188263

Carrette T, Alderslade P, Seymour J (2002) Nematocyst ratio and prey in two Australian cubomedusans, *Chironex fleckeri* and *Chiropsalmus* sp. Toxicon 40:1547–1551. doi:10.1016/S0041-0101(02)00168-X

Cimino G, Alfa M, La Spada G (1983) Trace elements in tentacles from the jellyfish *Pelagia noctiluca*. Mar Pollut Bull 14:197–198. doi:10.1016/0025-326X(83)90232-1

Cohen J (1988) Statistical power analysis for the behavioural sciences. Lawrence Erlbaum, Hillsdale

Colin SP, Costello JH, Katija K, Seymour J, Kiefer K (2013) Propulsion in cubomedusae: mechanisms and utility. PLoS One 8(2):e56393. doi:10.1371/journal.pone.0056393

Daverat F, Tomas J, Lahaye M, Palmer M, Elie P (2005) Tracking continental habitat shifts of eels using otolith Sr/Ca ratios: validation and application to the coastal, estuarine and riverine eels of the Gironde–Garonne–Dordogne watershed. Mar Freshw Res 56:619–627. doi:10.1071/MF04175

De Vries MC, Gillanders BM, Elsdon TS (2005) Facilitation of barium uptake into fish otoliths: influence of strontium concentration and salinity. Geochim Cosmochim Acta 69:4061–4072. doi:10.1016/j.gca.2005.03.052

Elsdon TS, Gillanders BM (2005) Consistency of patterns between laboratory experiments and field collected fish in otolith chemistry: an example and applications for salinity reconstructions. Mar Freshw Res 56:609–617. doi:10.1071/MF04146

Ferguson JE, Henderson GM, Kucera M, Rickaby REM (2008) Systematic change of foraminiferal Mg/Ca ratios across a strong salinity gradient. Earth Planet Sci Lett 265:153–166. doi:10.1016/j.epsl.2007.10.011

Gallahar NK, Kingsford MJ (1996) Factors influencing Sr/Ca ratios in otoliths of *Girella elevata*: an experimental investigation. J Fish Biol 48:174–186. doi:10.1111/j.1095-8649.1996.tb01111.x

Glass GV, Peckham PD, Sanders JR (1972) Consequences of failure to meet assumptions underlying the fixed effects analysis of variance and covariance. Rev Educ Res 42:237–288

Gordon M, Seymour J (2012) Growth, development and temporal variation in the onset of six *Chironex fleckeri* medusae seasons: a contribution to understanding jellyfish ecology. PLoS One 7(2):e31277. doi:10.1371/journal.pone.0031277

Gordon M, Hatcher C, Seymour J (2004) Growth and age determination of the tropical Australian cubozoan *Chiropsalmus* sp. Hydrobiologia 530(531):339–345. doi:10.1007/s10750-004-2655-7

Hamner WM, Jones MS, Hamner PP (1995) Swimming, feeding, circulation and vision in the Australian box jellyfish, *Chironex fleckeri* (Cnidaria: Cubozoa). Mar Freshw Res 46:985–990. doi:10.1071/MF9950985

Hartwick RF (1991) Distributional ecology and behaviour of the early life stages of the box-jellyfish *Chironex fleckeri*. Hydrobiologia 216(217):181–188. doi:10.1007/978-94-011-3240-4_25

Jack L, Wing SR, Hu Y, Roberts M (2011) Natural trace elemental markers for adult red rock lobsters *Jasus edwardsii* vary among replicate distinct water masses. Mar Ecol Prog Ser 443:141–151. doi:10.3354/meps09510

Jacups SP (2010) Warmer waters in the northern territory-herald an earlier onset to the annual *Chironex fleckeri* stinger season. EcoHealth 7:14–17. doi:10.1007/s10393-010-0306-1

Kawamura M, Ueno S, Iwanaga S, Oshiro N, Kubota S (2003) The relationship between fine rings in the statolith and growth of the cubomedusa *Chiropsalmus quadrigatus* (Cnidaria: Cubozoa) from Okinawa Island, Japan. Plankton Biol Ecol 50:37–42

Kingsford MJ, Mooney CJ (2014) The ecology of box jellyfishes (Cubozoa). In: Pitt KA, Lucas CH (eds) Jellyfish blooms. Springer, Netherlands, pp 267–302. doi:10.1007/978-94-007-7015-7_12

Kingsford MJ, Hughes JM, Patterson HM (2009) Otolith chemistry of the non-dispersing reef fish *Acanthochromis polyacanthus*: cross-shelf patterns from the central Great Barrier Reef. Mar Ecol Prog Ser 377:279–288. doi:10.3354/meps07794

Kingsford MJ, Seymour JE, O'Callaghan MD (2012) Abundance patterns of cubozoans on and near the Great Barrier Reef. Hydrobiologia 690:257–268. doi:10.1007/s10750-012-1041-0

Kraus RT, Secor DH (2004) Incorporation of strontium into otoliths of an estuarine fish. J Exp Mar Biol Ecol 302:85–106. doi:10.1016/j.jembe.2003.10.004

Marshall JF, McCulloch MT (2002) An assessment of the Sr/Ca ratio in shallow water hermatypic corals as a proxy for sea surface temperature. Geochim Cosmochim Acta 66:3263–3280. doi:10.1016/S0016-7037(02)00926-2

Martin GB, Thorrold SR (2005) Temperature and salinity effects on magnesium, manganese, and barium incorporation in otoliths of larval and early juvenile spot *Leiostomus xanthurus*. Mar Ecol Prog Ser 293:223–232. doi:10.3354/meps293223

Martin GB, Thorrold SR, Jones CM (2004) Temperature and salinity effects on strontium incorporation in otoliths of larval spot (*Leiostomus xanthurus*). Can J Fish Aquat Sci 61:34–42. doi:10.3354/meps293223

McClounan S, Seymour J (2012) Venom and cnidome ontogeny of the cubomedusae *Chironex fleckeri*. Toxicon 60:1335–1341. doi:10.1016/j.toxicon.2012.08.020

McCulloch M, Cappo M, Aumend J, Müller W (2005) Tracing the life history of individual barramundi using laser ablation MC-ICP-MS Sr-isotopic and Sr/Ba ratios in otoliths. Mar Freshw Res 56:637–644. doi:10.1071/MF04184

Miles NG, West RJ, Norman MD (2009) Does otolith chemistry indicate diadromous lifecycles for five Australian riverine fishes? Mar Freshw Res 60:904–911. doi:10.1071/MF08252

Mooney CJ, Kingsford MJ (2012) Sources and movements of *Chironex fleckeri* medusae using statolith elemental chemistry. Hydrobiologia 690:269–277. doi:10.1007/s10750-012-1049-5

Morse JW, Bender ML (1990) Partition coefficients in calcite: examination of factors influencing the validity of experimental results and their application to natural systems. Chem Geol 82:265–277. doi:10.1016/0009-2541(90)90085-L

Nilsson DE, Gislén L, Coates MM, Skogh C, Garm A (2005) Advanced optics in a jellyfish eye. Nature 435:201–205. doi:10.1038/nature03484

Paton C, Hellstrom J, Paul B, Woodhead J, Hergt J (2011) Iolite: freeware for the visualisation and processing of mass spectrometric data. J Anal At Spectrom 26:2508–2518. doi:10.1039/C1JA10172B

Phillis CC, Ostrach DJ, Ingram BL, Weber PK (2011) Evaluating otolith Sr/Ca as a tool for reconstructing estuarine habitat use. Can J Fish Aquat Sci 68:360–373. doi:10.1139/F10-152

Sadovy Y, Severin KP (1992) Trace elements in biogenic aragonite: correlation of body growth rate and strontium levels in the otoliths of the white grunt, *Haemulon plumieri* (Pisces: Haemulidae). Bull Mar Sci 50:237–257

Sanchez-Jerez P, Gillanders BM, Kingsford MJ (2002) Spatial variability of trace elements in fish otoliths: comparison with dietary items and habitat constituents in seagrass meadows. J Fish Biol 60:801–821. doi:10.1111/j.1095-8649.2002.tb00912.x

Secor DH, Henderson-Arzapalo A, Piccoli PM (1995) Can otolith microchemistry chart patterns of migration and habitat utilisation in anadromous fishes? J Exp Mar Biol Ecol 192:15–33. doi:10.1016/0022-0981(95)00054-U

Seymour JE, Carrette TJ, Sutherland PA (2004) Do box jellyfish sleep at night? Med J Aust 181:707

Sötje I, Neues F, Epple M, Ludwig W, Rack A, Gordon M, Boese R, Tiemann H (2011) Comparison of the statolith structures of *Chironex fleckeri* (Cnidaria, Cubozoa) and *Periphylla periphylla* (Cnidaria, Scyphozoa): a phylogenetic approach. Mar Biol 158:1149–1161. doi:10.1007/s00227-011-1637-3

Strasser CA, Mullineaux LS, Thorrold SR (2008) Temperature and salinity effects on elemental uptake in the shells of larval and juvenile softshell clams *Mya arenaria*. Mar Ecol Prog Ser 370:155–169. doi:10.3354/meps07658

Tabouret H, Bareille G, Claverie F, Pécheyran C, Prouzet P, Donard OFX (2010) Simultaneous use of strontium:calcium and

barium:calcium ratios in otoliths as markers of habitat: application to the European eel (*Anguilla anguilla*) in the Adour basin, South West France. Mar Environ Res 70:35–45. doi:10.1016/j.marenvres.2010.02.006

Tanner SE, Reis-Santos P, Vasconcelos RP, Fonseca VF, Franca S, Cabral HN, Thorrold SR (2013) Does otolith geochemistry record ambient environmental conditions in a temperate tidal estuary? J Exp Mar Biol Ecol 441:7–15. doi:10.1016/j.jembe.2013.01.009

Templeman MA, Kingsford MJ (2010) Trace element accumulation in *Cassiopea* sp. (Scyphozoa) from urban marine environments in Australia. Mar Environ Res 69:63–72. doi:10.1016/j.marenvres.2009.08.001

Templeman MA, Kingsford MJ (2012) Variation in soft tissue chemistry among scyphozoan and cubozoan jellyfishes from the Great Barrier Reef, Australia. Hydrobiologia 690:279–290. doi:10.1007/s10750-012-1051-y

Thébault J, Chauvaud L, L'Helguen S, Clavier J, Barats A, Jacquet S, Pécheyran C, Amouroux D (2009) Barium and molybdenum records in bivalve shells: geochemical proxies for phytoplankton dynamics in coastal environments? Limnol Oceanogr 54(3):1002–1014. doi:10.4319/lo.2009.54.3.1002

Tibballs J (2006) Australian venomous jellyfish, envenomation syndromes, toxins and therapy. Toxicon 48:830–859. doi:10.1016/j.toxicon.2006.07.020

Tiemann H, Sötje I, Becker A, Jarms G, Epple M (2006) Calcium sulfate hemihydrate (bassanite) statoliths in the cubozoan *Carybdea* sp. Zool Anz 245:13–17. doi:10.1016/j.jcz.2006.03.001

Tzeng WN (1996) Effects of salinity and ontogenetic movements on strontium: calcium ratios in the otoliths of Japanese eel, *Anguilla japonica* Temminick and Schlegel. J Exp Mar Biol Ecol 199:111–122. doi:10.1016/0022-0981(95)00185-9

Ueno S, Imai C, Mitsutani A (1995) Fine growth rings found in statolith of a cubomedusa *Carybdea rastonii*. J Plankton Res 17:1381–1384. doi:10.1093/plankt/17.6.1381

Underwood AJ (1997) Experiments in ecology: their logical design and interpretation using analysis of variance. Cambridge University Press, Cambridge **504 pp**

Walther BD, Kingsford MJ, O'Callaghan MD, McCulloch MT (2010) Interactive effects of ontogeny, food ration and temperature on elemental incorporation in otoliths of a coral reef fish. Environ Biol Fish 89:441–451. doi:10.1007/s10641-010-9661-6

Wang CH (2014) Otolith elemental ratios of flathead mullet *Mugil cephalus* in Taiwanese waters reveal variable patterns of habitat use. Estuar Coast Shelf Sci 151:124–130. doi:10.1016/j.ecss.2014.08.024

Watanabe T, Kiron V, Satoh S (1997) Trace minerals in fish nutrition. Aquaculture 151:185–207. doi:10.1016/S0044-8486(96)01503-7

Watson EB (1996) Surface enrichment and trace-element uptake during crystal growth. Geochim Cosmochim Acta 60(24):5013–5020. doi:10.1016/S0016-7037(96)00299-2

Woodhead JD, Hellstrom J, Hergt JM, Greig A, Maas R (2007) Isotopic and elemental imaging of geological materials by laser ablation Inductively Coupled Plasma-mass spectrometry. Geostand Geoanal Res 31:331–343. doi:10.1111/j.1751-908X.2007.00104.x

Zacherl DC, Manríquez PH, Paradis G, Day RW, Castilla JC, Warner RR, Lea DW, Gaines SD (2003) Trace elemental fingerprinting of gastropod statoliths to study larval dispersal trajectories. Mar Ecol Prog Ser 248:297–303. doi:10.3354/meps248297

Zumholz K, Hansteen TH, Piatkowski U, Croot PL (2007) Influence of temperature and salinity on the trace element incorporation into statoliths of the common cuttlefish (*Sepia officinalis*). Mar Biol 151:1321–1330. doi:10.1007/s00227-006-0564-1